



Research Article

Axial Compression Behavior of Recycled Concrete Filled Steel Tubular Short Columns after High Temperature

Xiao Liu ^{1,2}, Siying Liu ¹, Yanchuan Hui,^{1,3} Xuexin Zhang,¹ Bing Wang,¹ and Lei Zhao¹

¹Shenyang University, 21 Wanghai South Street, Shenyang 110044, China

²Shenyang Key Laboratory of Intelligent Disaster Prevention and Mitigation of Civil Buildings, 21 Wanghai South Street, Shenyang 110044, China

³Wuhan University, 8 Eastlake Street, Wuhan 430072, China

Correspondence should be addressed to Xiao Liu; liuxiao@syu.edu.cn

Received 6 April 2022; Revised 25 May 2022; Accepted 6 September 2022; Published 23 September 2022

Academic Editor: Claudio Mazzotti

Copyright © 2022 Xiao Liu et al. This is an open access article distributed under the Creative Commons Attribution License, which permits unrestricted use, distribution, and reproduction in any medium, provided the original work is properly cited.

This article is devoted to study the axial compression behaviour of recycled concrete-filled steel tubular (RCFST) columns after high temperature. Several axial compression members' internal mechanisms are analyzed by combining experimental and finite element analysis (FEA). Firstly, the failure mode of axial compression members is studied by experiments. Then, based on the correct constitutive relationship between recycled concrete and steel, the finite element model is established by ABAQUS software, and theoretical analysis and experimental verification are carried out, which are in good agreement. The effects of different parameters such as temperature, substitution rate, and bond strength of the coefficient on the whole load-strain curve are compared. The results show that the bearing capacity of recycled concrete-filled steel tubular columns decreases with the increase in temperature and replacement rate. The bond coefficient between steel tubular and core concrete has little effect on the specimen's overall axial compressive mechanical properties. The interaction force P rises slightly along the height after the high temperature at the peak load, as it gradually moves away from the cover. In the square section, corners show stress concentration, and bulge deformation occurs first under the condition of axial compression.

1. Introduction

Recycled concrete-filled steel tubular (RCFST) columns not only retain the high bearing capacity and seismic capacity of concrete-filled steel tubulars but also are environmental-friendly. RCFST is widely used in engineering sectors [1–3]. Recycled concrete is made by crushing and cleaning the waste concrete, replacing the old aggregate wholly or partly with natural aggregate according to a certain gradation level, and then recompounding it into concrete. The use of recycled concrete can effectively save natural aggregates and reduce the impact of waste concrete on the ecological environment, so it has a good application prospect.

Scholars have carried out many experimental studies on the mechanical properties of recycled concrete structures at room temperature and have obtained a series of research results [4–7]. In recent years, various types of building fire

incidents have occurred frequently, and the mechanical properties of structural members after fires are an essential basis for the safety assessment and damage repair of buildings. Therefore, the mechanical properties of recycled concrete-filled steel tubular columns after high temperature still need to be further studied. Yang et al. [8] analyzed the failure process of the steel tubular recycled short concrete column after high temperature and proposed the change law of the interaction between the steel tubular and the core recycled concrete during the stress process. Wang et al. [9] analyzed the effect of different parameters on the steel tubular after high temperature. The effect of recycled concrete on mechanical properties was explained. The factors affecting the reduction coefficient of axial compression bearing capacity after high temperature were explained.

By comparing the calculating result of a finite element to experiments, this paper shows a correct axial compression

model for recycled concrete-filled steel tubular columns after the high temperature. The influence of different parameters on the mechanical properties of recycled concrete-filled steel tubular after the high temperature is revealed, and the working mechanism and interference between steel tube and recycled concrete are revealed. This paper provides a reference for further in-depth study and engineering application of recycled concrete-filled steel tubular.

2. Test Overview

In order to further understand the mechanical properties of recycled concrete-filled steel tubular under axial compression after high temperature. In this experiment, three recycled concrete-filled steel tubular columns with a 100% substitution rate were tested. The main parameters of the test were temperature (20°C, 300°C, and 600°C). The specimens' details are shown in Table 1. Firstly, the three specimens were put into a box-type resistance furnace and kept in the center of the furnace. Then the furnace's temperature was raised to the target temperature (between 300°C and 600°C), and the target temperature was kept for 3 hours to ensure the uniformity of the members' temperature. Finally, open the door so that specimens can cool to room temperature naturally, and the specimens were taken out. After the high-temperature test, axial compression tests were carried out on a 500 t press.

2.1. Specimen Material. Q345 manganese steel were used as the steel. Through a tensile test, the measured average yield strength (f_y) was 358 MPa and the ultimate strength (f_u) was 520 MPa. The elastic modulus (E_s) and the Poisson's ratio (ν_s) of steel were 203000 MPa and 0.298, respectively. The testing machine and standard specimen are shown in Figure 1.

The concrete material was Gongyuan Brand 425 Ordinary Portland Cement, the fine aggregate was ordinary natural river sand, and the coarse aggregate was the waste concrete after crushing, sieving, and cleaning to obtain a continuous graded recycled coarse aggregate. The particle size range was 5–25 mm. The water was ordinary tap water, and the water-reducing agent was a naphthalene-based superplasticizer with a water-reducing rate of 0.125. Recycled concrete was proportioned according to the strength of C70 natural concrete, and recycled coarse aggregates were used to completely replace natural aggregates, namely cement: sand: coarse aggregate: water = 1:1.05:2.22:0.28. Table 2 is the recycled concrete component content and measured strength. As shown in Table 2, the compressive strength of the concrete cubes was measured by three sets of standard 150 × 150 × 150 mm standard cube blocks under the condition of 28 d curing. In this test, the measured average strength (f_{cu}) was 38.25 MPa.

2.2. Design of Specimens. During the production of the test piece, one end of the steel tube was sealed, and circular holes with a diameter of 12 mm were reserved on the surface of the steel tube so that the test piece could discharge the water vapor of the recycled concrete during high-temperature heating. Then, the stirred and poured the concrete materials

evenly into the steel tube according to the proportion, vibrated until the concrete surface was uniform and flat, and maintained it under standard conditions for 28 days. The residual concrete on the surface of the exhaust hole was cleaned up, and a cover plate was welded on the other end of the steel tube.

2.3. Heating up of the Specimen. This test used a box-type resistance furnace. The maximum heating temperature of the resistance furnace was 960°C, and the furnace size was 800 × 760 × 660 mm. According to the different heating temperatures, the three specimens were heated, respectively. The specimens were laid flat in the furnace, and the temperature was kept constant for 3 hours when the temperature reached the predetermined temperature (300°C and 600°C). During the heating process, when the temperature reaches 250°C, the sound of water vapor discharging outward can be clearly heard. When the temperature rises to 380°C or continues to heat for a period of time, the sound gradually disappears. After heating, the specimen was cooled naturally and taken out. It was found that when the heating temperature was 300°C, the specimen's surface color did not change significantly. When the temperature was 600°C, the specimen's surface was slightly red when it came out of the furnace. After cooling, the surface was oxidized, and the appearance became obviously red.

2.4. Loading Device and Settings. The loading was carried out on a 500 t press. The position of the loading device, strain gauge, and displacement gauge are shown in Figure 2. Before the test, the surface of the test piece was polished and smooth. To accurately obtain the deformation of the test piece, strain gauges were set at equal distances in the cross section and circumferential directions of the test piece, and two mutually perpendicular strain gauges were installed on the side. The axial and transverse strains of the test piece were measured, respectively. The loading method was manual loading. During the initial loading process, the loading speed was uniform. When the specimen reached the peak load, the loading speed was slowed down, and the loading was stopped when the specimen axially deformed 20 mm.

2.5. Failure Mode Analysis. It can be seen from Figure 3 that under the condition of axial compression, the failure mode of the RCFST after the high temperature is similar to that of the RCFST at room temperature. At the initial stage of the specimen loading, the specimen was basically in the elastic stage, and the outer surface of the specimen had no obvious deformation. As the load increased, the specimen locally entered the plastic deformation stage, the shear slip line began to appear in the middle of the steel tube surface, and the oxide layer on the surface of the steel tube fell off, and as the load increased, the shear slip line also gradually increased. As the axial deformation increased, the surface of the steel tube began to buckle locally. As shown in the figure, the oxide layer on the surface of the steel tube fell off, the

TABLE 1: Specific parameters of each specimen in the test.

Data sources	Test piece	$D/(mm)$	$t/(mm)$	$L/(mm)$	$R/(%)$	$T/(^{\circ}C)$	$f_y/(MPa)$	$f_{cu}/(MPa)$	$N_{ue}/(kN)$	$N_l/(kN)$	N_l/N_{ue}
Paper test	S-R4-20	150	3	450	100	20	358	38.25	1580.54	1640.15	1.022
	S-R4-300	150	3	450	100	300	358	38.25	1682.25	1644.01	0.977
	S-R4-600	150	3	450	100	600	358	38.25	1374.97	1396.87	1.016



FIGURE 1: Testing machine and standard specimen.

specimen entered the failure stage, the local concrete was crushed, and the loading of the specimen ended.

3. Numerical Modelling and Verification

3.1. Model Description. The finite element (FE) model for the RCFST member was developed to simulate the failure mode, the contact stress, as well as the loads carried by steel tube and concrete. A comprehensive model was established, and the steel tube and the concrete were modelled separately and connected by contact relationships.

In this model, the steel tube was modelled by a four-node shell element and the concrete was modelled by an eight-node solid element, respectively. The constitutive model of steel after a constant high temperature can be expressed as [10]

$$\sigma = \begin{cases} E_s(T) \cdot \varepsilon, & (\varepsilon \leq \varepsilon_y(T)), \\ f_y(T) + E'_s(T) \cdot [\varepsilon - \varepsilon_y(T)], & (\varepsilon > \varepsilon_y(T)), \end{cases} \quad (1)$$

where $E_s(T)$ is the elastic modulus of steel after constant temperature. $E'_s(T)$ is the steel's elastic modulus in the strengthening stage. $E'_s(T) = 0.01E_s(T)$. $\varepsilon_y(T)$ is the yield strain of steel after constant high temperature. The yield strength of steel after the constant high temperature is calculated according to the following formula [10]:

$$f_y(T) = \begin{cases} f_y, & (T \leq 400^{\circ}C), \\ \lambda \cdot f_y, & (T > 400^{\circ}C). \end{cases} \quad (2)$$

Based on the uniaxial constitutive relationship model of modified replacement rate and the maximum temperature experienced in [11], the constitutive model of concrete, the peak stress and peak strain after high temperature were substituted for the peak stress and peak strain relationship at room temperature:

$$\sigma_0(T) = \frac{\sigma_0}{(1 + 6.4\alpha_T^{3.9})},$$

$$\varepsilon_0(T) = \varepsilon_0 \left[1 + (1500T + 5T^2) \times 10^{-6} \right], \quad (3)$$

$$\alpha_T = \frac{(T - 20)}{1000},$$

where $\sigma_0(T)$ and σ_0 are the peak stress after high temperature and normal temperature respectively; $\varepsilon_0(T)$ and ε_0 are peak strain after high temperature and at room temperature, respectively. The cracking stress of concrete is 10% of peak stress. The value of tensile fracture energy is determined by the method in [12]:

$$G_f = 0.26(1.25f'_c)^{2/3} \left(1 - \frac{t}{1000} \right). \quad (4)$$

A surface-based interaction model was used for the contact behaviour between steel tube and recycled concrete. In the tangential direction and the normal direction, the Coulomb friction model and the hard-contact model were used, respectively. The frictional factor (μ) was taken to be 0, 0.3 and 0.6, respectively, in this analysis, where $\mu = 0$ and $\mu = 0.6$ were considered as unbonded and fully bonded, respectively.

When meshing, the edge layout was used to mesh the members. The load adopted the displacement loading method: rigid constraints were imposed on the bottom cover of the model without any corners or displacements. The top cover plate limited the rotation angle in X, Y, and Z directions and the displacement in X and Y directions. The specimen only had axial displacement in the Z direction, as shown in Figure 4.

3.2. Verification. In order to verify the correctness of the finite element model, the finite element models of three recycled concrete-filled steel tubular specimens in this paper and the specimens in Reference [13] were established respectively, and the model operation results were compared with the experimental results. Table 3 is the specific parameters of specimens in Reference [13].

The specimens' specific parameters and the comparison results are shown in Table 1, where N_{ue} is the test peak load, and N_l is the peak load calculated by the finite element method. Figure 5 shows the comparison of load-strain curves between this paper's calculated results and the test results of the specimens. The finite element curve in the elastic phase coincides with the test curve; the ultimate load and the peak longitudinal strain are also basically the same, the curve of the descending section after the ultimate load and the finite element simulation curve. Consistent with the overall downward trend of the test result curve, the average

TABLE 2: Content of each component and measured strength of recycled concrete.

Substitution rate (%)	Concrete material consumption (kg/m ³)				Cube compressive strength of specimen (MPa)			
	Cement	Recycled coarse aggregate	Fine aggregate	Water (kg/m ³)	Test piece 1	Test piece 2	Test piece 3	Average value
100	550	1221	575	154	59.87	25.81	37.07	38.25

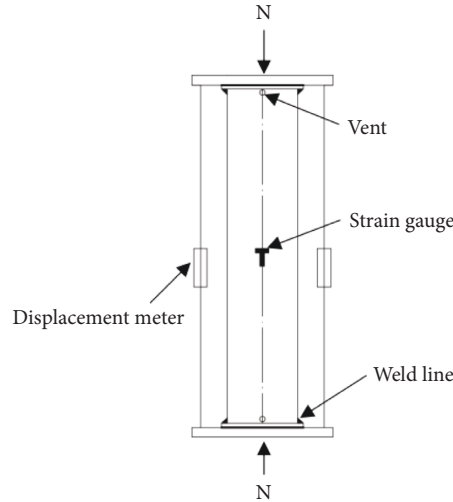


FIGURE 2: Loading device.

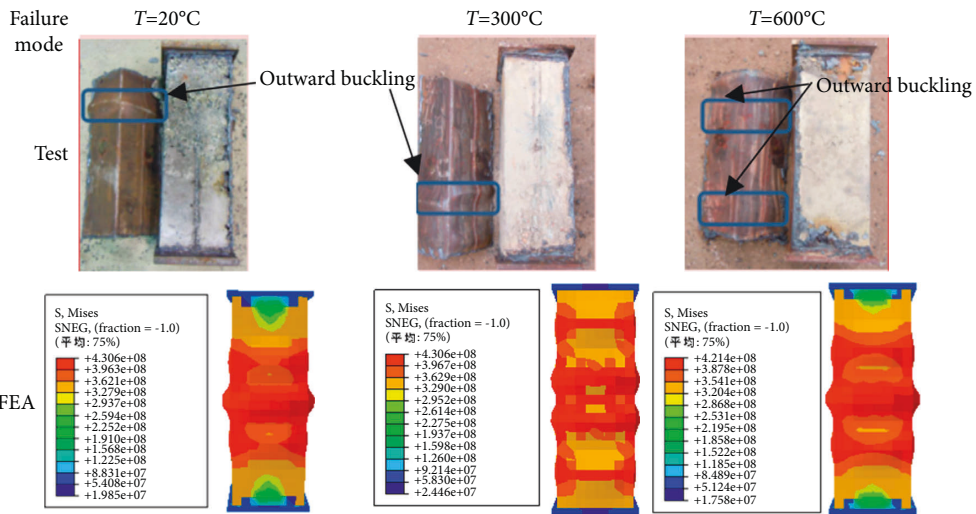


FIGURE 3: Failure mode of specimens.

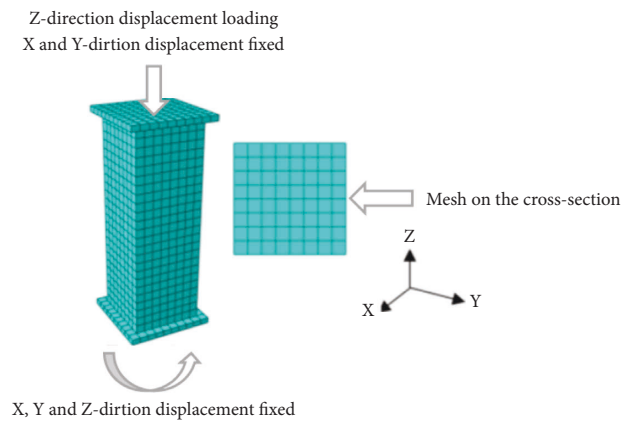


FIGURE 4: Mesh division and constraint loading mode.

TABLE 3: Specific parameters of each specimen in the literature.

Data sources	Test piece	$D/(mm)$	$t/(mm)$	$L/(mm)$	$R/(%)$	$T/(^{\circ}C)$	$f_y/(MPa)$	$f_{cu}/(MPa)$	$N_{ue}/(kN)$	$N_l/(kN)$	N_l/N_{ue}
Literature [13]	S1-20	120	6	360	50	20	176.5	53.3	856.44	875.61	1.022
	S1-300	120	6	360	50	300	176.5	53.3	815.95	873.45	1.070
	S1-600	120	6	360	50	600	176.5	53.3	571.32	585.06	1.024

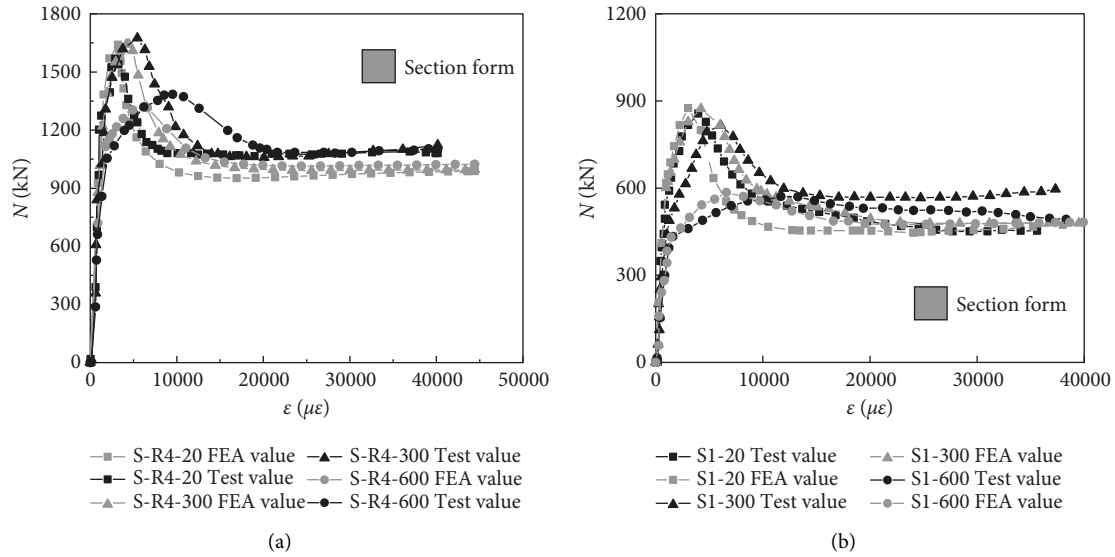


FIGURE 5: Comparison of test curve with FEA in this paper. (a) Comparison between the test in this paper and FEA results. (b) Comparison of test in reference [13] and FEA results.

value of the ratio of the simulated value to the test value is 1.022. It can be seen from the figure that the calculation of this order value is in good agreement with the test curve as a whole, the model establishment is relatively reasonable, and the force analysis of the specimen is relatively accurate.

4. Finite Element Analysis

A short column model of recycled concrete-filled steel tubular under high temperature was built through the finite element software ABAQUS. The size of the model was 120 mm × 360 mm × 3 mm. The concrete strength ratio was 70 Mpa, the steel strength was 345 Mpa, and both ends of the model were covered. The board adopted a 150 mm × 150 mm square cover. The parameters of the specimen were selected as the highest historical temperature T (20°C, 300°C, 600°C, and 800°C), substitution rate (0%, 50%, 100%). At the same time, for consideration, the influence of the interaction strength between the steel tube and the core recycled concrete on the mechanical properties of the specimen, the bond strength coefficient was selected as ($\mu=0, 0.3, 0.6$) in this paper. Figure 6 shows the influence of the parameters on the load-displacement curve.

4.1. Parameter Analysis

4.1.1. The Influence of Temperature. Figure 6 shows the load-displacement deformation curves of recycled concrete-filled steel tubular specimens at different historical maximum temperatures. The force and deformation of recycled

concrete-filled steel tubular are similar to that of ordinary concrete-filled steel tubular; the overall load-displacement curve shows a linear growth stage, a nonlinear growth stage, and a slow-growth stage the descending phase. At the same substitution rate, the specimen's peak load decreases with the increase of temperature, the specimen's axial stiffness decreases with the increase of temperature, and the peak strain generally increases with the increase of temperature.

Figure 7 is the effect of temperature on the ultimate bearing capacity of recycled concrete-filled steel tubular under different replacement ratios. It can be seen that after high temperature, square concrete-filled steel tube short columns decreased by 2.0% on average at 300°C, decreased by 27.4% on average at 600°C, decreased by 56.2% on average at 800°C; Overall, the temperature below 600°C has little effect on the specimens' bearing capacity, and the ultimate load of specimens above 600°C decreases greatly. This is because with the increase in temperature, the crystal water inside the concrete gradually evaporates under the action of high temperature, and the loss of mechanical properties after high temperature is basically irreversible. Therefore, the higher the temperature, the greater the reduction of its own strength and elastic modulus. The strength of steel is also lost due to high temperature, but the steel will recover large material loss strength after high temperature cooling. During the loading process, the strength of the core concrete decreases and the axial deformation increases. Due to the constraint effect of steel tube on core concrete, the specimen shows good ductility at the later stage of the curve.

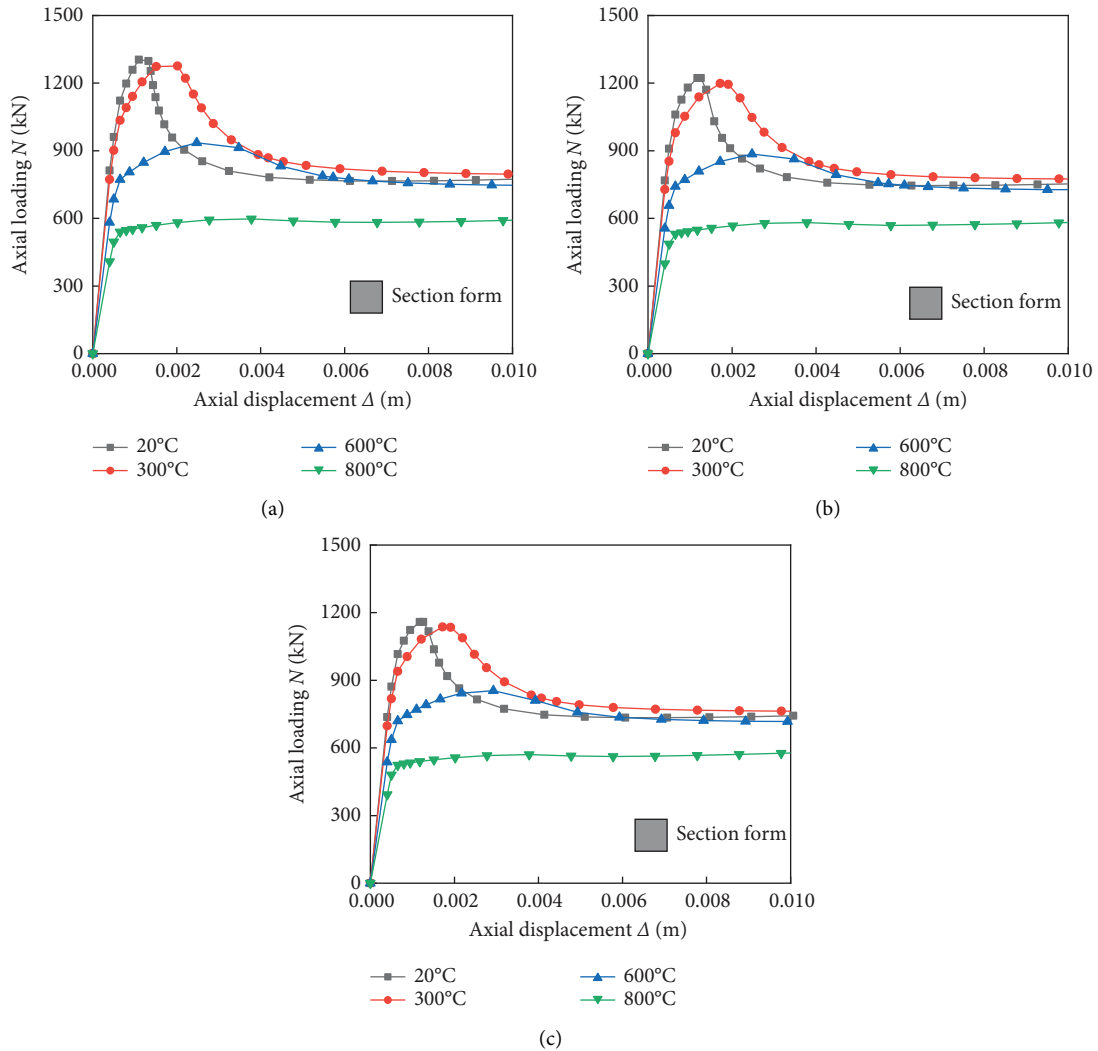


FIGURE 6: Load-deformation relationship curve. (a) $r=0\%$. (b) $r=50\%$. (c) $r=100\%$.

4.1.2. The Influence of Replacement Rate. Figure 8 is the influence of replacement ratio on specimens' ultimate bearing capacity at different temperatures. Compared with $r=0\%$, the specimens' ultimate bearing capacity with $r=50\%$ and $r=100\%$ decreases by 6.3% and 11.1%, respectively. At $T=20^\circ\text{C}$ and $T=300^\circ\text{C}$, the specimens' ultimate bearing capacity decreased by 6.0% and 10.9%, respectively. When $T=600^\circ\text{C}$, it decreases by 5.4% and 8.7%, respectively. When $T=800^\circ\text{C}$, the ultimate bearing capacity of the specimens is hardly affected by the substitution rate.

In Figure 8, the specimens' overall peak load decreases as the replacement rate increases. The reason is that the mechanical properties of recycled concrete are lower than those of ordinary concrete, but based on the good high-temperature resistance of recycled concrete, its mechanical properties are lower than those of ordinary concrete under high temperature. Therefore, the specimens' bearing capacity decreases slightly with the increase in substitution rate. At the same time, due to the material performance loss of the core concrete after high temperature, with the increase in temperature, the ratio of the bearing capacity of the core

concrete and the steel tube to the total bearing capacity decreases, and the influence of the replacement rate on the bearing capacity of the specimen gradually decreases.

4.2. The Influence of the Cohesive Coefficient. The interaction between steel tubes and concrete is transmitted through the interface between them. However, scholars have researched the factors affecting the bonding strength, and few studies on the bond strength affecting the axial compression performance of recycled concrete-filled steel tubular [14]. Therefore, to study the influence of bond strength, referring to the research method of Johansson [15], three friction coefficients (μ) of 0, 0.3, and 0.6 were adopted in the finite element calculation and analysis.

Figure 9 shows the specimen's load-strain curve under different bonding coefficients. From the figure, the change in the bond strength has little effect on the elastic phase of the curve. The steel tube and the core concrete are evenly stressed in the elastic phase, and no relative slip has occurred. Due to the local buckling deformation of the steel and the crushing of

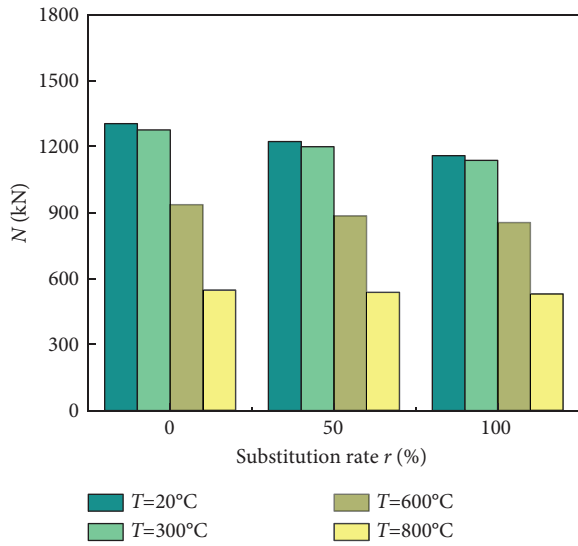


FIGURE 7: Influence of temperature on ultimate bearing capacity.

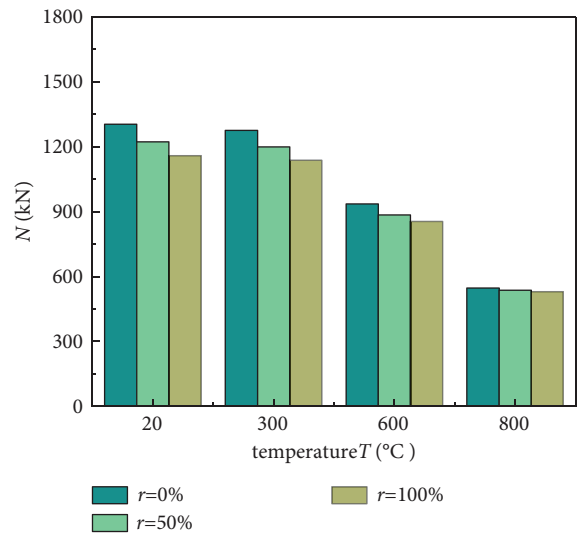


FIGURE 8: Influence of substitution rate on ultimate bearing capacity.

the concrete, the relative slip between the steel tube and the core concrete is affected by the bond coefficient. The specimen's ultimate bearing capacity will increase slightly with the increase of the bond coefficient, but the magnitude of the influence is much smaller than the influence of the substitution rate and temperature on the test piece.

Figure 10 is the histogram of specimens' ultimate bearing capacity with different bond strength coefficients. It can be seen from the figure that with the increase of the bond coefficient under the same substitution rate, the specimen's ultimate bearing capacity shows a slight upward trend. When the bonding coefficient $\mu = 0.3$ compared with $\mu = 0$, the specimen's ultimate bearing capacity increased by about 0.21% on average. When the bonding coefficient $\mu = 0.6$ is compared with that of $\mu = 0.3$, the specimen's ultimate load-bearing capacity increases by about 0.02% on average; at the same temperature, the bonding coefficient $\mu = 0.3$ compared

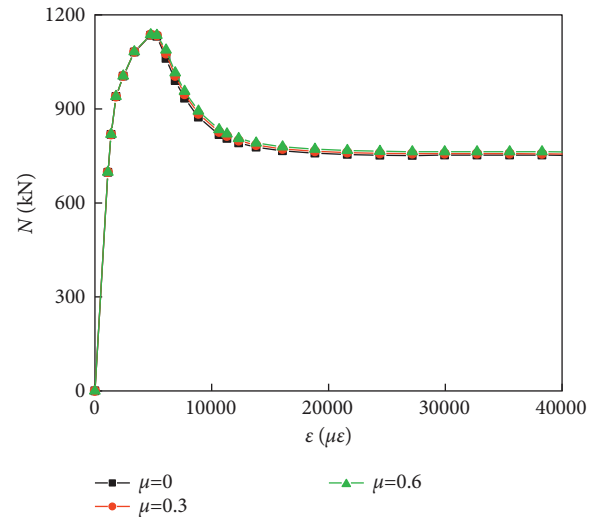


FIGURE 9: N - ϵ relationship curve between bond strength and ultimate bearing capacity.

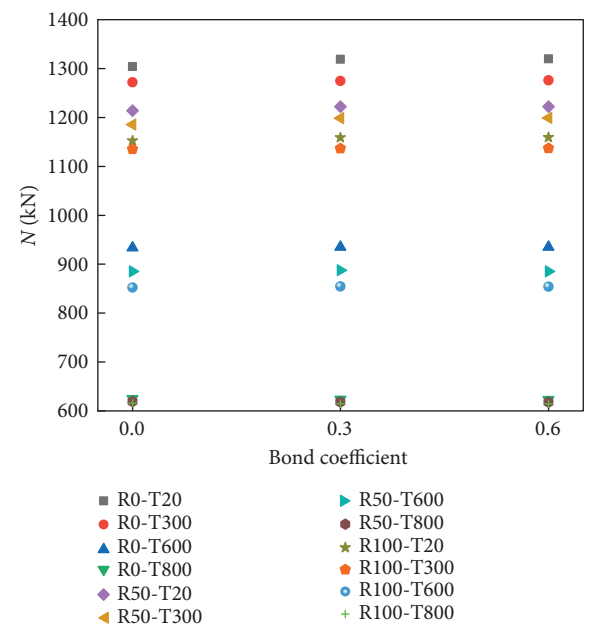


FIGURE 10: Influence of bond strength coefficient on ultimate bearing capacity.

with $\mu = 0$, the average increase in the specimen's ultimate bearing capacity is about 0.52%; the adhesion coefficient $\mu = 0.6$ compared with the case of $\mu = 0.3$, the average increase in the specimen's ultimate bearing capacity is about 0.13%. For the recycled concrete-filled steel tubular specimens, with the increase of the bond strength coefficient, the interaction between the core concrete and the steel tube is improved so that the specimens' ultimate bearing capacity increases slightly. However, compared with the influence of temperature and substitution rate factors, it can be considered that the cohesive coefficient has little effect on the axial compressive properties of the specimen in the joint action of the steel tube and the core concrete under the axial compressive load.

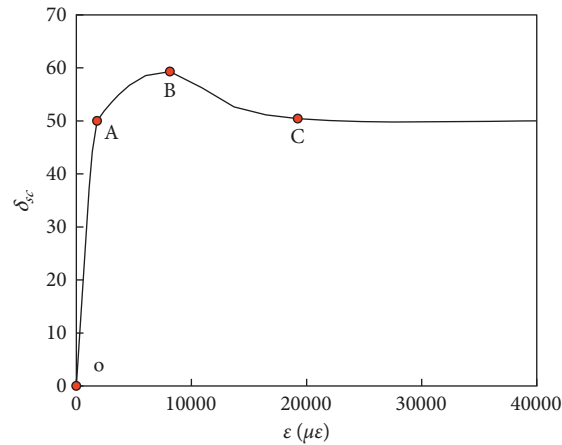


FIGURE 11: Typical $\delta_{sc} - \epsilon$ curves of members.

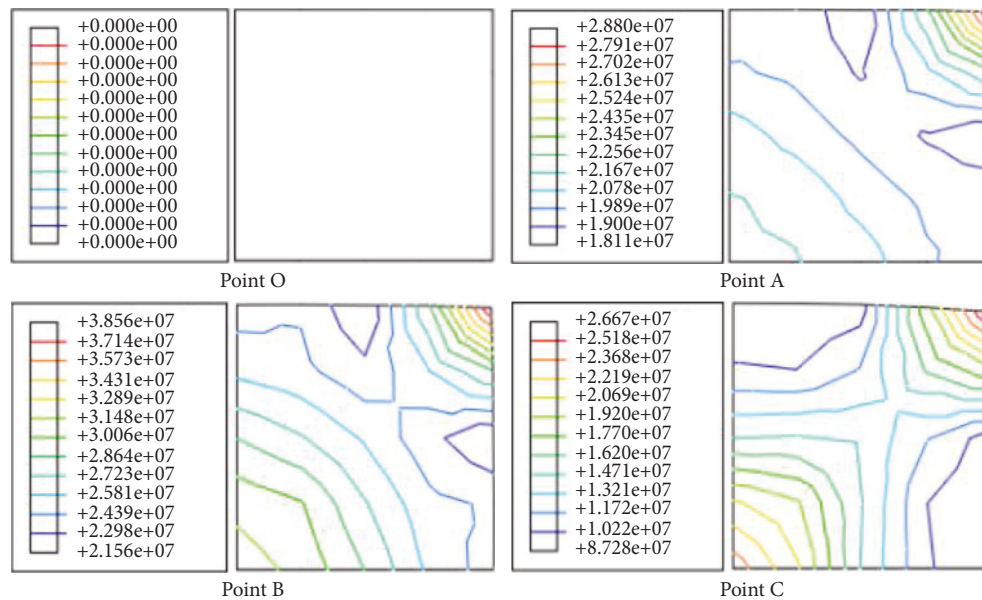


FIGURE 12: Stress distribution map of concrete midspan section.

4.3. Mechanism Analysis. The axial pressure of recycled concrete-filled steel tube after high-temperature is analyzed. Recycled concrete-filled steel tubular column with a replacement rate of 100% and a historical maximum temperature of 600°C. Figure 11 shows the typical curves of members. The abscissa represents strain, and the ordinate represents the nominal compressive stress of members. The four characteristic points are selected on the typical curve this time, namely O (initial point, the specimen is about to enter the axial compression force), A (endpoint of the elastic stage, the steel tube enters the elastoplastic stage), B (specimen reaches the ultimate load point), and C (the longitudinal strain of the specimen reaches 0.02).

Figure 12 is the stress distribution map of the concrete midspan section. Figures 11 and 12 show that: In the OA stage, the whole specimen is in the elastic growth stage. At point A of the specimen, the strong restraint effect of the corner steel tube, so stress concentration occurs.

In the AB stage, the specimen enters the elastoplastic stage, and the axial stress of the specimen continues to increase until point B reaches the peak stress. Due to the influence of substitution rate and high temperature, the specimen's peak load is lower than the standard value of the compressive strength of ordinary concrete cylinders. From the stress-strain curve of the steel tube, it can be found that the AB section steel tube has not yet yielded, due to the restraint effect of the steel tube, the corner stress concentration is apparent, and the concrete core stress growth is not apparent.

At section BC, when the specimen enters the plastic stage, while the longitudinal strain increases, the corner stress of the steel tube decreases.

Figure 13 shows the variation of load-bearing capacity of steel tubes and concrete with longitudinal strain after high temperature. It can be seen from the figure that with the increase of the specimen's longitudinal strain, the ultimate

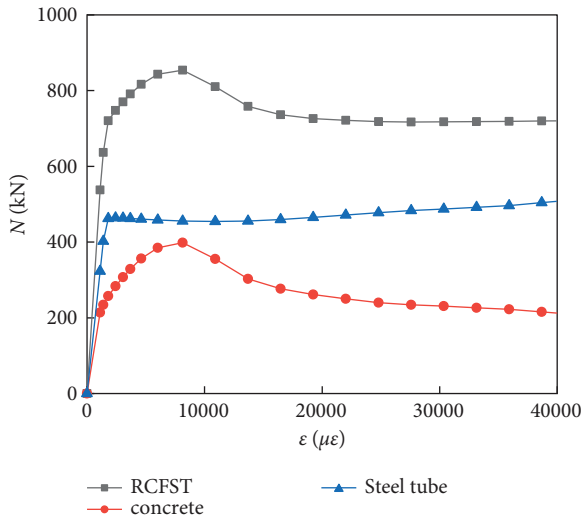


FIGURE 13: Load proportion diagram of components in RCFST.

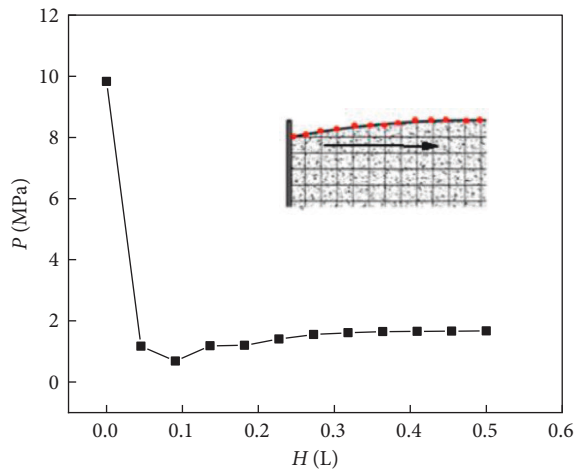


FIGURE 14: Change of P along member height when RCFST reaches peak load after high temperature.

bearing capacity varies with the core concrete reduced by deformation and failure, and the bearing capacity of the core recycled concrete decreases from 59.1% to 38.2%. The steel tube's bearing capacity increases in the later stage of failure, and the specimen shows good ductility performance in the plastic decline section.

The interaction force between the steel tube and the concrete is considered in the analysis. It is assumed that the average binding force between the steel tube and the concrete is P . Because the interaction force P of the square section specimen is not uniform, the average contact pressure of the whole section is taken. Because the specimen is symmetrical about the middle section, the binding force of steel tube on core concrete is also symmetrical about the middle section. Figure 14 shows the change in the height of P along with the member when the recycled concrete-filled steel tubular column reaches the peak load after a high temperature. Due to the more significant restraint effect of the fixed end of the cover plate, the square steel tube specimen here shows a sizeable restraining force P . At the

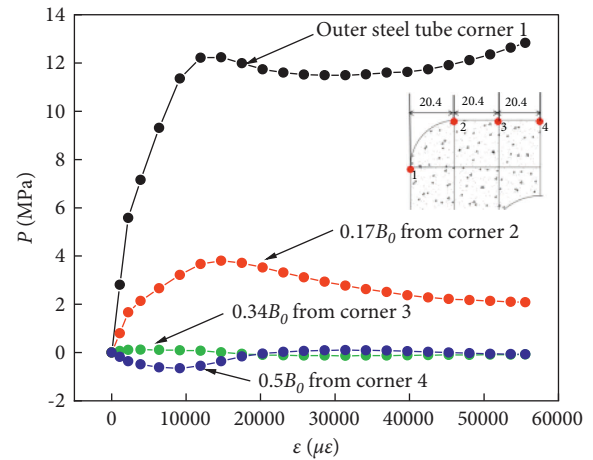


FIGURE 15: Change of restraining force at different positions of the section in member.

distance from the cover plate, the contact pressure between the steel tube and the concrete after the high temperature is at the peak load. As it gradually moves away from the cover, it rises slightly in the height direction.

Figure 15 shows the binding force between the steel tube and the core recycled concrete at different positions of the specimen's middle section after high temperature. In Figure 15, in different positions of the specimen, the contact stress value P is the largest at the corner, and it decreases with the increase of the distance from the corner. The contact pressure at the middle of the section edge basically tends to zero, and the later contact pressure is even negative. Therefore, the corner shows the phenomenon of stress concentration under axial compression, and bulge deformation occurs.

5. Conclusion

In this paper, the bearing capacity degradation law of recycled concrete-filled steel tubular columns under the influence of different parameters was analyzed by combining experimental and finite element analysis. The following conclusions are obtained as follows:

- (1) The deformation of recycled concrete-filled steel tubular after high temperature is similar to that of ordinary concrete-filled steel tubular column. The curve changes linearly in the early stage of loading. After entering the elastoplastic stage, the member's axial stiffness drops rapidly, and the member buckles and fails. With the member's bearing capacity shows a downward trend, the rise in temperature and the increase in replacement rate.
- (2) The temperature has a significant influence on the member's ultimate bearing capacity. The higher the historical temperature, the more significant the decrease in the bearing capacity and the higher the ratio of the steel tube's bearing capacity to the total bearing capacity. Therefore, it exhibits good ductility

performance in the later stage. The ultimate bearing capacity shows a downward trend with the increase in the replacement rate. With the increase in temperature, the influence of the replacement rate will gradually decrease. When $T = 800^{\circ}\text{C}$, the specimen's ultimate bearing capacity is hardly affected by the substitution rate.

- (3) Under axial compression, with the increase of bond strength, the interaction force between steel tube and core concrete increases, and the specimen's ultimate bearing capacity increases slightly, but it has little effect on the overall axial compression mechanical properties of the specimen.

Data Availability

Data are available on request to the authors.

Conflicts of Interest

The authors declare that they have no conflicts of interest.

Acknowledgments

The authors gratefully acknowledge the support provided by the National Natural Science Foundation of China (52078306); Youth Science Foundation Project (12102269); Science and Technology Plan Project of Shenyang City (21-108-9-21) and Natural Fund Guidance Plan (2019-ZD-0538); and the support of Shenyang Youth Science and Technology Innovation Talent Support Program (RC190380).

References

- [1] W. Li, Z. Luo, Z. Tao, W. H. Duan, and S. P. Shah, "Mechanical behavior of recycled aggregate concrete-filled steel tube stub columns after exposure to elevated temperatures," *Construction and Building Materials*, vol. 146, pp. 571–581, 2017.
- [2] Y. C. Tang, L. J. Li, W. X. Feng, F. Liu, and M. Zhu, "Study of seismic behavior of recycled aggregate concrete-filled steel tubular columns," *Journal of Constructional Steel Research*, vol. 148, pp. 1–15, 2018.
- [3] V. W. Y. Tam, Z. B. Wang, and Z. Tao, "Behaviour of recycled aggregate concrete filled stainless steel stub columns," *Materials and Structures*, vol. 47, no. 1-2, pp. 293–310, 2014.
- [4] Y. Liu, X. Zha, and G. Gong, "Study on Recycled-Concrete-Filled Steel Tube and recycled concrete based on damage mechanics," *Journal of Constructional Steel Research*, vol. 71, pp. 143–148, 2012.
- [5] W. H. Choi, J. H. Lee, Y. P. Park, S. H. Kim, and S. M. Choi, "Compressive performance of 50MPa concrete filled square and circular steel tubes(CFT) columns using recycled aggregate," *Journal of the Korean Society for Advanced Composite Structures*, vol. 9, no. 2, pp. 72–80, 2018.
- [6] H. Ma, J. Dong, G. B. Hu, and Y. Liu, "Axial compression performance of composite short columns composed of RAC-filled square steel tube and profile steel," *Journal of Constructional Steel Research*, vol. 153, pp. 416–430, 2019.
- [7] Y. C. Tang, L. J. Li, W. X. Feng, F. Liu, and B. Liao, "Seismic performance of recycled aggregate concrete-filled steel tube columns," *Journal of Constructional Steel Research*, vol. 133, pp. 112–124, 2017.
- [8] Y. F. Yang, Z. C. Zhang, and F. Fu, "Experimental and numerical study on square RACFST members under lateral impact loading," *Journal of Constructional Steel Research*, vol. 111, no. 8, pp. 43–56, 2015.
- [9] B. Wang, L. Xiao, L. Zhao, and G. Lu, "Analysis of axial compression performance of recycled concrete filled steel tube short columns at high temperature," *Engineering Mechanics*, vol. 32, no. S1, pp. 153–158, 2015.
- [10] L. Han, *Concrete-Filled Steel Tube Structure* Science Press, Beijing, 2016.
- [11] J. F. Wang, L. H. Han, and B. Uy, "Hysteretic behaviour of flush end plate joints to concrete-filled steel tubular columns," *Journal of Constructional Steel Research*, vol. 65, no. 8-9, pp. 1644–1663, 2009.
- [12] Ministry of Housing and Urban-Rural Development of the People's Republic of China, *Standard for Design of Steel Structures: GB50017-2017* China Planning Press, Beijing, 2017.
- [13] Y. Yang and R. Hou, "Theoretical analysis and experimental research on short steel tube recycled concrete columns after high temperature," *Journal of Disaster Prevention and Mitigation Engineering*, vol. 32, no. 01, pp. 71–76, 2012.
- [14] W. Q. Lyu and L. H. Han, "Investigation on bond strength between recycled aggregate concrete(RAC)and steel tube in RAC-filled steel tubes," *Journal of Constructional Steel Research*, vol. 155, 2019.
- [15] M. Johansson, "Structural behavior of circular steel-concrete composite columns: non-linear finite element analyses and experiments," Licentiate thesis, Chalmers University of Technology, Div. of concrete Struct, Goteborg, Sweden, 2000.